第 27卷 第 1期 焊 接 学 报 Vol 27 No. 1
2006年 1月 TRANSACTIONS OF THE CHINA WELDING INSTITUTION January 2006

双丝间接电弧氩弧焊的熔滴过渡

曹梅青， 邹增大， 杜宝帅， 曲仕尧
（山东大学 材料科学与工程学院，济南 250061）

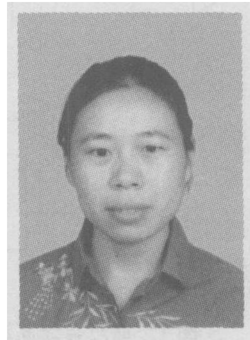
曹梅青

摘 要：采用氙灯背光高速摄像系统及示波器对双丝间接电弧氩气保护焊的熔滴过渡及其对应的电压、电流波形进行了研究。结果表明，双丝间接电弧氩弧焊焊接电流与电弧电压的不同匹配选择，熔滴具有短路过渡、大滴过渡、混合过渡、射滴过渡、射流过渡等不同过渡形式。随着焊接电流的增大熔滴尺寸减小，熔滴细化，随电弧电压的增大，熔滴尺寸减小。熔滴过渡形式与电压、电流的波形之间有很好的对应关系。

关键词：间接电弧；熔滴过渡；短路过渡；射流过渡
中图分类号：TG444+.72 文献标识码：A 文章编号：0253-360X(2006)01-45-04

0 序 言

熔滴过渡是非常重要的焊接过程。它不仅决定着焊条、焊丝的工艺性能，而且影响电弧的稳定性，与焊缝质量有着密切的关系。国内外学者对熔化极气体保护焊（GMAW）[1~4]和药芯焊丝电弧焊（FCAW）[5,6]的熔滴过渡进行了大量的研究。熔化极气体保护焊熔滴自由过渡又分为大滴过渡、喷射过渡及爆炸过渡，大滴过渡包括大滴滴落过渡和大滴排斥过渡，喷射过渡包括射滴过渡、射流过渡和旋转射流过渡[7]。王其隆[8]对熔化极气体保护焊熔滴自由过渡形式的特征和实质进行了详细的介绍。实心焊丝埋弧焊通常把熔滴过渡分为自由过渡、接触过渡及渣保护过渡[9]。

双丝间接电弧气体保护焊是一种新的焊接工艺。其两焊丝分别接电源的正、负极，工件不接电源，焊接时在两焊丝端部间形成单一电弧。虽然双电极焊条单弧焊跟该焊接方法类同，但其熔滴过渡形式并不相同[10]。迄今为止关于双丝间接电弧气体保护焊熔滴过渡的报道很少。而开展双丝间接电弧气体保护焊熔滴过渡研究，对于从本质上认识该焊接方法的焊接工艺性，提高焊接熔敷率及焊接质量具有十分重要的意义。

1 试 验

1.1 试验材料

试验用焊丝为直径 ϕ1.2 mm的 H08Mn2SiA，用氩气作为保护气体。为了便于观察，采用在离工件较远处燃烧法和平板堆焊方法研究双丝间接电弧气体保护焊熔滴过渡形态。平板堆焊时试验用母材为Q235钢，尺寸为 200 mm×100 mm×3 mm。焊接以前用砂轮将试板表面打磨干净，防止铁锈、油污影响焊接质量。

1.2 试验设备和方法

试验用焊机为 NBC-350型逆变式 CO_2气体保护焊焊接电源，具有微升的外特性。所用焊接电压 29~33 V。送丝机为 2台额定电压 DC 24 V、额定电流 5A 的 AS系列送丝机，负极用原单丝焊时的等速送丝反馈电路来控制负极送丝，正极采用作者专门设计的送丝机构来控制正极送丝[11]。用 Agilent 54624A示波器测试双丝间接电弧气体保护焊时的电弧电压和焊接电流波形。示波器和高速摄像系统采用同步触发控制。采用氙灯背光高速摄像方法研究双丝间接电弧气体保护焊的熔滴过渡。为了去除强烈的弧光干扰，用氙灯作为背光光源。用 TIG焊机串联上一个电容作为氙灯的电源，通过调节电流的大小来调节氙灯的光强。氙灯光路及高速摄像系统如图 1所示。氙灯是利用凹面镜原理来工作的，将灯泡放在凹面镜的焦距处，这样可以得到一束平行光，用此光束照射电弧而得到焊丝和熔滴过渡的影像。弧光通过滤光片被滤除。为了提高图像质量，在焊丝与滤光片之间安装一个与摄像头大小相近的小孔。采用 FASTCAM Super-10KC型高速摄像机拍摄熔滴过渡图像，最高拍摄速度为10 000帧/s。文中选用 1 000帧/s的拍摄速度拍摄熔滴过渡，两焊丝所在平面与摄像方向垂直。在焊接过程中，每次拍摄时间为 2.1 s。拍摄的熔滴图片

收稿日期：2005-06-07
基金项目：山东省自然科学基金资助项目（Z2002F03）
*参加此项研究工作的还有王新洪，李德刚

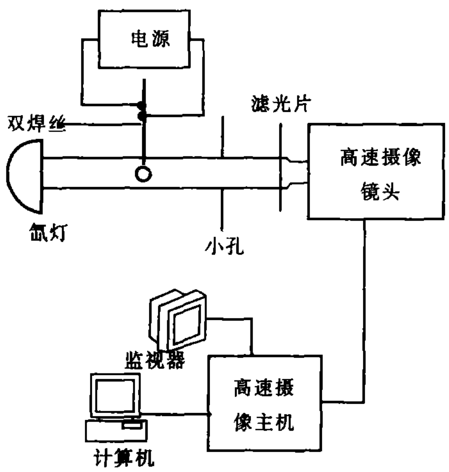

图 1 氙灯背光高速摄像系统示意图

Fig. 1 Xenon lamp optics and high speed camera system

传送到计算机,存储在硬盘中,用通用的看图软件对熔滴过渡图片进行观察和分析。

2 试验结果和讨论

2.1 焊接电流对双丝间接电弧氩弧焊熔滴过渡的影响

电压 33V,不同电流下的各种过渡形式如图 2所示。图中所示的间隔为每两幅图片之间的时间间隔。

由图 2可以看出,随着焊接电流的增大,阴、阳极熔滴的尺寸都减小,电流变化相同时,阳极熔滴的尺寸变化更为显著,由大熔滴变为比较细小的熔滴。

焊接电流不同,熔滴过渡的形式也有所不同。

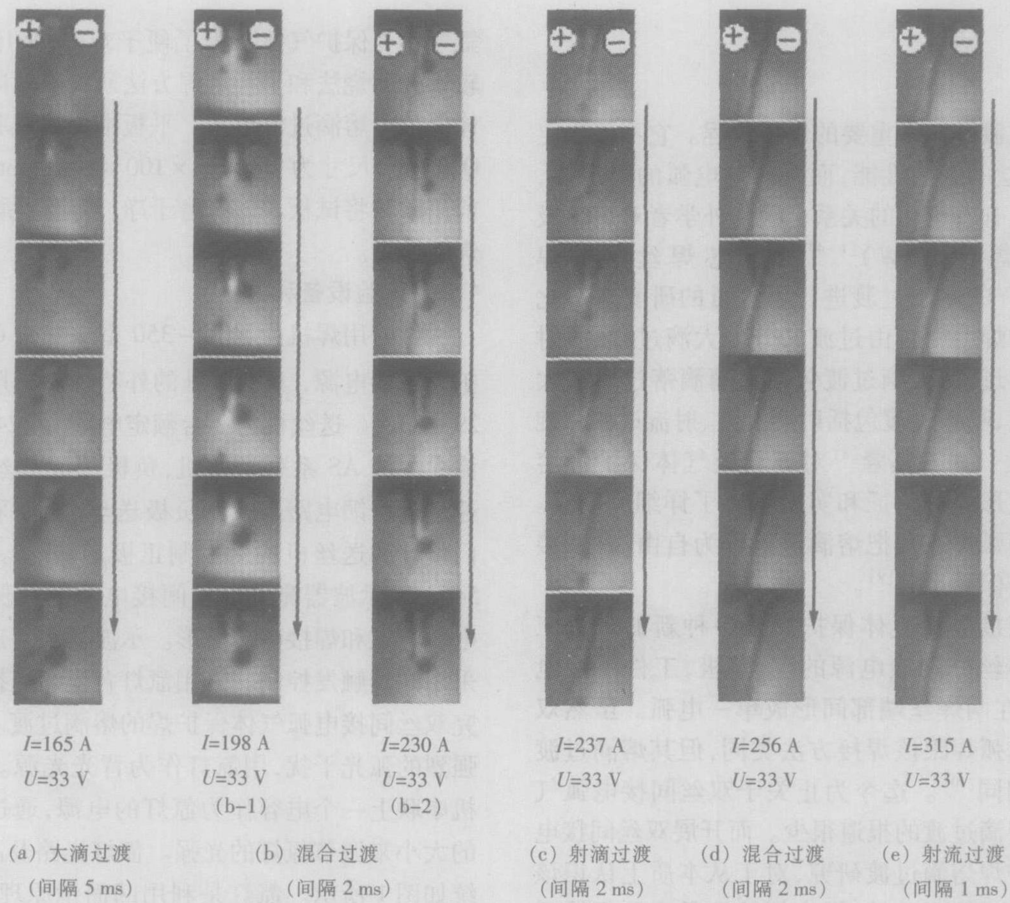

图 2 双丝间接电弧氩弧焊不同电流下的熔滴过渡形式

Fig. 2 Metal transfer of twin-wire indirect arc argon welding with different welding current

电流为 165A 时出现大滴过渡,如图 2a所示。此时弧根面积小于熔滴直径,电磁力不易使熔滴形成缩颈,而斑点压力又阻碍熔滴过渡。随着焊丝的熔化,熔滴不断长大,当其重力克服表面张力的作用形成大滴进行过渡时,由于阴阳极斑点压力的不同,所形成的熔滴大小也有所不同,负极熔滴的尺寸比正极熔滴更大。

随电流的增大,熔滴受到的电磁收缩力增大,熔滴变细。但由于阴、阳极斑点力的不同,阴极的熔滴受到更大的阻碍熔滴过渡的力,故其要在更大的电流下完成射流过渡,如图 2b所示。当电流为 198 A 时,阳极为射滴过渡,阴极为大滴过渡 (图 2b-1);

当电流为 230 A时,阳极为射流过渡,阴极为大滴过渡 (图 2b –2)。这两种过渡形式称为混合过渡。

当电流增大到 237 A时,出现射滴过渡(图 2c)。过渡时,熔滴直径接近于焊丝直径,脱离焊丝沿焊丝轴向过渡。射滴过渡时弧根面积扩大并包围熔滴,使斑点压力和电磁收缩力都利于熔滴过渡,只有表面张力对熔滴过渡起阻碍作用。在这种情况下,熔滴容易下落,并被电磁收缩力、等离子流力、重力等加速,形成射滴过渡。这时熔滴下落的加速度大于重力加速度。

当电流为 256 A时,阳极为射流过渡,阴极为射滴过渡 (图 2d)。这是由于阳极熔滴在电磁收缩力、等离子流力、重力等的作用下,已达到形成射流的条件,而由于阴极斑点力较大,其仍为射滴过渡。这种过渡形式阴、阳极的过渡形式也不相同,故也称其为混合过渡。

当电流进一步增大到 315 A时,电磁收缩力较大,弧根不但完全包围了熔滴,而且还扩展到熔滴的缩颈以上,容易形成较强的等离子流,使焊丝端部的液态金属呈"铅笔尖"状,这种过渡形式为射流过渡 (图 2e)。

综上所述,随着焊接电流的增大,熔滴的过渡形式为大滴过渡 – –混合过渡 – –射流过渡。这是因为电流越大电磁收缩力越大,并且弧根的分布也发生变化,促使熔滴过渡的力越多,从而熔滴越容易过渡。

2.2 电弧电压对熔滴过渡的影响

电弧电压对熔滴过渡的影响示于图 3。由图 3可以看出,当电压较小时容易出现短路过渡,如图 3a所示。与一般的单丝焊短路过渡不同的是,双丝间接电弧焊的短路过程是指两焊丝相接触而短路,而不是熔滴与熔池接触的短路。

随着电弧电压的增大,熔滴的尺寸减小,过渡频率增加,熔滴细化。阳极焊丝的过渡形式发生明显改变,从短路过渡 – –大滴过渡 – –射滴过渡 – –射流过渡;阴极焊丝的过渡形式从短路过渡变为大滴过渡后就不再发生明显改变,但熔滴颗粒变小。这主要是由于电压越高,用于熔化焊丝的能量越多,从而使熔滴变得细小。

2.3 电流、电压与熔滴的过渡形式

电流、电压不同,熔滴的过渡形式也发生明显的改变。随着焊接电流及电弧电压的增大,熔滴由短路过渡 – –大滴过渡 – –混合过渡 – –射滴过渡 – –射流过渡。

电弧电压、焊接电流的波形图与熔滴过渡之间有着密切的关系,图 4为 30 ms内熔滴过渡与其电流、电压的对应关系图。

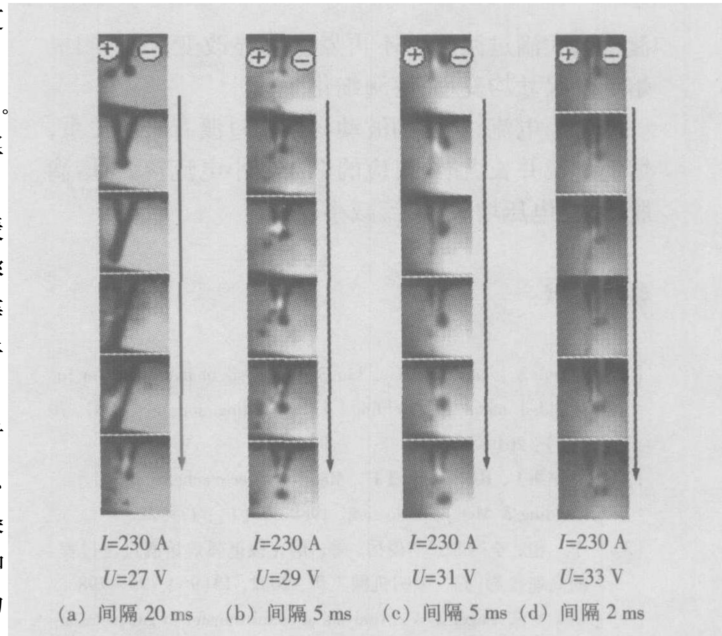

图 3　电弧电压对熔滴过渡的影响

Fig. 3　Influence of arc voltage on metal transfer

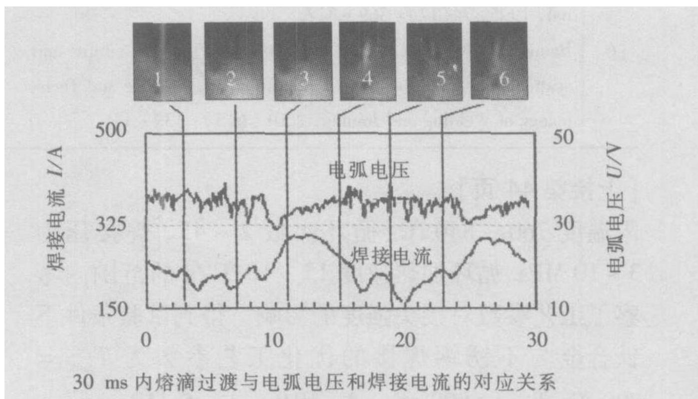

图 4　熔滴过渡与电弧电压和焊接电流的关系

Fig. 4　Corresponding relation between metal transfer and arc voltage and welding current

由图 4可以看出,在熔滴形成并长大的过程中电弧电压是逐渐减小的而对应的焊接电流则增大 (如图 4中图片 2、3、5所示)。这是由于随着熔滴的长大,两焊丝端部之间的距离减小,电弧变短,电弧电压降低。当熔滴脱离焊丝向熔池过渡时 (如图 4中图片 1、4、6所示),由于两焊丝端部间距离增大,电弧变长,电弧电压升高,对应的焊接电流降低。

3　结　　论

(1) 双丝间接氩弧焊焊接电流对熔滴过渡影响较大,随着焊接电流的增大,熔滴的过渡形式发生改变,并且熔滴变得细小。

(2) 随电弧电压的增大,双丝间接氩弧焊阳极的熔滴过渡形式为短路过渡 – –大滴过渡 – –射滴过渡 – –射流过渡;阴极焊丝的过渡形式从短路过

渡变为大滴过渡后就不再发生明显改变。阴、阳极熔滴的尺寸均变小,熔滴细化。

(3)电流、电压的波动与熔滴过渡有密切关系,熔滴形成并长大时,对应的电压较小电流较大;熔滴脱落时,电压增大,电流减小。

参考文献:

[1] Brandi S, Taniguchi C, Liu S. Analysis of metal transfer in shielded metal arc welding[J]. Welding Journal, 1991, 70(10): 261-270.

[2] Norrish J, Richardson I F. Metal transfer mechanisms[J]. Welding & Metal Fabrication, 1988, 56(1): 17-22

[3] 李 桓, 李国华, 李俊岳, 等. 熔化极电弧焊熔滴过渡过程的高速摄影[J]. 中国机械工程, 2002, 13(9): 796-798

[4] Kim Y S, Eager T W. Analysis of metal transfer in gas metal arc welding[J]. Welding Journal, 1993, 72(6): 269s-278s

[5] Wang W, Liu S, Jones J E. Flux core arc welding: arc signals processing and metal transfer characterization[J]. Welding Journal, 1995, 74(12): 369-377.

[6] Baune E, Bonnet C, Liu S. Assessing metal transfer stability and spatter severity in flux cored arc welding[J]. Science and Technology of Welding and Joining, 2001, 6(3): 139-148.

[7] Anon. Classification of metal transfer on arc electric welding process[J]. Welding in the World, 1977, 15(5-6): 113-117.

[8] 姜焕中. 电弧焊及电渣焊[M]. 北京: 机械工业出版社, 1995.

[9] Wang Qilong, Yin Shuyan, Zhang Jiuhai, et al. About the classification and the chinese designation of the metal transfer modes of free flight in MIG welding[J]. Transctions of the China Welding Institution, 1983, 4(3): 149-154
王其隆, 殷树言, 张九海, 等. 关于熔化极气体焊熔滴自由过渡的分类与名称问题[J]. 焊接学报, 1983, 4(3): 149-154.

[10] Han Bin, Zou Zengda, Qu Shirao, et al. Metal transfer and ist influence factor of lime titania type twin electrodes[J]. Transactions of the China Welding Institution, 2004, 25(5): 63-66
韩 彬, 邹增大, 曲仕尧, 等. 双电极钛钙型焊条熔滴过渡及其影响因素[J]. 焊接学报, 2004, 25(5): 63-66.

[11] 王春茂, 曹梅青, 邹增大, 等. 双丝单弧气体保护焊工艺[J]. 焊接技术, 2005, 34(2): 35-37.

作者简介:曹梅青, 女, 1977年出生, 博士研究生。现从事新材料及连接技术的研究工作, 发表论文 10篇。

Email: cmq@mail.sdu.edu.cn

[上接第 44页]

限温度 760~840 ℃、循环次数 2~45、焊接压力 3~10 MPa、循环加热速度 15~10 ℃/s的范围内考察了工艺参数对接头强度的影响。得到试验条件下钛合金与不锈钢焊接的优化工艺参数为 $T_{max}=890$ ℃, $T_{min}=800$ ℃, $N=10$, $p=5$ MPa, $v_h=30$ ℃/s。在此工艺条件下,接头强度达到 307 MPa,而焊接时间仅为 160 s。

(2)钛合金与不锈钢扩散焊接接头从不锈钢侧开始依次形成了 σ、Fe_2Ti、FeTi和 β-Ti层,在不锈钢侧还形成了少量的 NiTi。拉伸试验时,接头沿 FeTi和 β-Ti层之间的某一个位置断裂, β-Ti承受了主要的拉力,而 FeTi金属间化合物层是接头的薄弱环节。

参考文献:

[1] Ghosh M, Bhanumurthy K, Kale G B, et al. Diffusion bonding of titanium to 304 stainless steel[J]. Journal of Nuclear Materials, 2003, 322(2-3): 235-241.

[2] Orhan N, Khan T I, Eroglu M. Diffusion bonding of a microduplex stainless steel to Ti-6Al-4V[J]. Scripta Materialia, 2001, 45(4): 441-446.

[3] He P, Feng J C, Zhang B G, et al. Microstructure and strength of diffusion bonded joints of TiAl base alloy to steel[J]. Materials Characterization, 2002, 48(5): 401-406

[4] Calvo F A, Urena A, Gomez De Salazor J M, et al. Special features of the formation of the diffusion bonded joints between copper and aluminium[J]. Journal of Materials Science, 1988, 23(6): 2273-2280

[5] Ghosh M, Chatterjee S. Diffusion bonded transition joints of titanium to stainless steel with improved properties[J]. Materials Science and Engineering, 2003, A358(1-2): 152-158

[6] Andrzejewski H, Badawi K F, Rolland B. Roughness in the diffusion welding of Ti-6Al-4V alloy[J]. Welding Research Supplement, 1993, (9): 435-439.

[7] Maehara Y, Komizo Y, Langdon T G. Principles of superplastic bonding[J]. Materials Science and Technology, 1988, 4(8): 669-674.

[8] Kato H, Shibata M, Yoshikawa K. Diffusion welding of Ti/Ti and Ti/stainless steel rods under phase transformation in air[J]. Materials Science and Technology, 1986, 2(4): 405-409.

[9] Zhou Ronglin, Zhang Jiuhai, Tian Xitang. The effect of thermal cycle on joint of Ti/stainless steel phase transformation diffusion bonding[J]. China Welding, 2001, 10(1): 14-18.

[10] Aleman B, Gutierrez I, Urcola J J. The use of kirkendall effect for calculating intrinsic diffusion coefficients in a 316L/Ti6242 diffusion bonded couple[J]. Scripta Materialia, 1997, 36(5): 509-515

作者简介:秦 斌, 男, 1978年 5月出生, 博士研究生。现从事钛合金与不锈钢的扩散焊接研究工作, 发表论文 8篇。

Email: jjjjenny@163.com

welded surface microstructure of steel before welding. If only one surface is eligible for ultra-fining, the tensile strength of the joint will be also up to that of 40Cr base metal, but the welding time is slightly longer. ISSW belongs to the little deformation welding, the deformation of joint is mainly located in the quenched area near original interface. The deformation of T10A side is larger than that of 40Cr side.

Key words: steel; microstructure; ultra-fining treatment; super plastic solid-state welding process

Phase transformation diffusion bonding technology for titanium alloy to stainless steel

QIN Bin[1], SHENG Guang-min[1,2], HUANG Jia-wei[1], LI Cong[2] (1. College of Material Science and Engineering, Chongqing University, Chongqing 400044, China; 2. National Key Laboratory for Nuclear Fuel and Material, Nuclear Power Institute of China, Chengdu 610041, China). p41 – 44, 48

Abstract: The joints of titanium alloy (TA17) and stainless steel (0Cr18Ni9Ti) were obtained by phase transformation diffusion bonding. Effect of parameters on strength of the joint was investigated, and the optimum parameters for bonding are as follows: maximum cyclic temperature is 890 ℃, minimum cyclic temperature is 800 ℃, number of cyclic times is 10, bonding pressure is 5 MPa and heating velocity is 30 ℃ /s. Strength of the joint under the optimum condition is 307 MPa, and the time for bonding is 160 s. Scanning electron microscopy (SEM), energy dispersive spectroscopy (EDS) and X-ray diffraction (XRD) were used to study the fracture appearance of the joint. The study showed that the fracture takes place at somewhere between FeTi and β-Ti layers, and the FeTi layer is the weakest point in the joints. The joint was analyzed by EDS and the ternary phase diagram for Fe-Cr-Ti. The results indicated the presence of σ, Fe_2Ti, FeTi and β-Ti in the reaction zone between stainless steel and titanium alloy.

Key words: titanium alloy; stainless steel; phase transformation; diffusion bonding

Metal transfer of twin-wire indirect arc argon welding

CAO Mei-qing, ZOU Zeng-da, DU Bao-shuai, QU Shi-yao, WANG Xin-hong, LI De-gang (School of Material Science and Engineering, Shandong University, Jinan 250061, China). p45 – 48

Abstract: The metal transfer and the corresponding arc voltage and welding current in twin-wire indirect arc argon welding was investigated with high speed camera system based on a xenon lamp source and digital oscillograph. Results showed that with the different matching of welding current and arc voltage, the mode of metal transfer consists of short circuiting transfer, globular transfer, mixing transfer, projected transfer and streaming transfer etc. With the increasing of welding current, the droplet size reduces, and the droplet is refined. With the raising of arc voltage, the size of droplet reduces. There is well corresponding relationship between metal transfer mode and the oscillogram of volgtage and welding.

Key words: indirect arc; metal transfer; short circuiting transfer; streaming transfer

Autonomous seam tracking based on local vision in arc robotic welding

ZHOU Lü, CHEN Shan-ben, LIN Tao, CHEN Wen-jie (Welding Institue, Shanghai Jiaotong University, Shanghai 200030, China). p49 – 52

Abstract: A method of autonomous seam tracking in arc robotic welding was presented. It could make the robot get rid of traditional teaching and playing back mode and automatically acquired the special coordinates of welding seam. The master computer continuously processed local area images in front of the torch in the images which were acquired by a CCD camera to measure the deviation between the torch and the seam and the orientation of the seam. At the same time, the computer controlled the robot to make the torch move forward along the seam and recorded the seam ′s coordinates in the robotic basic reference frame which were corrected by the deviations. After the torch arrives at the end point of the seam, the computer controlled the robot to move the torch to the first record coordinate and begin to weld. Experiments were made on the curves seam workpieces of mild steel and aluminum alloy workpieces. The result showed that this method has good practicability.

Key words: image processing; arc welding robot; autonomous seam tracking; local vision

Distribution of Au during reaction of eutectic SnPb solder and Au/Ni/Cu pad

LI Fu-quan[1], WANG Chun-qing[1], DU Miao[2] (1. National Key Laboratory of Adranced Welding Production Technology, Harbin Institute of Technolog, Harbin 150001, China; 2. Harbin Welding Institute, Harbin 150080, China). p53 – 56

Abstract: Solder bump was fabricated with Sn-Pb eutectic solder droplet on Au/Ni/Cu pad. The solder/pad was then subject to reflow soldering and aging at 125 ℃. The IMC evolution at solder/pad interface during this process, especially the formation and distribution of Au-Sn compound were investigated. The results showed that Au-Sn compound forms at solder/pad interface during contact reaction, and Au does not react fully with solder droplet. During the subsequent reflow soldering, all Au layer at interface is consumed. Ni layer reacts with solder, which leads to the formation of Ni_3Sn_4 compound at the interface. Acicular $AuSn_4$ can be found in the solder bulk. $AuSn_4$ particles redesposites at the interface as a continuously $(Au_xNi_{1-x})Sn_4$ layer during aging at 125 ℃. The redesposited $(Au_xNi_{1-x})Sn_4$ at solder/pad interface follows decomposition-diffusion mechanism. At the same time, a lead-rich phase emerges with $AuSn_4$ redeposition at the interface. The shear strength of soldered joint is mainly determined by this evolution and distribution of Au-Sn compound.

Key words: solder bump; Au/Ni/Cu; reflow; ageing; interme